Soft Matter

Accepted Manuscript

ROYAL SOCIETY OF CHEMISTRY

www.rsc.org/softmatter

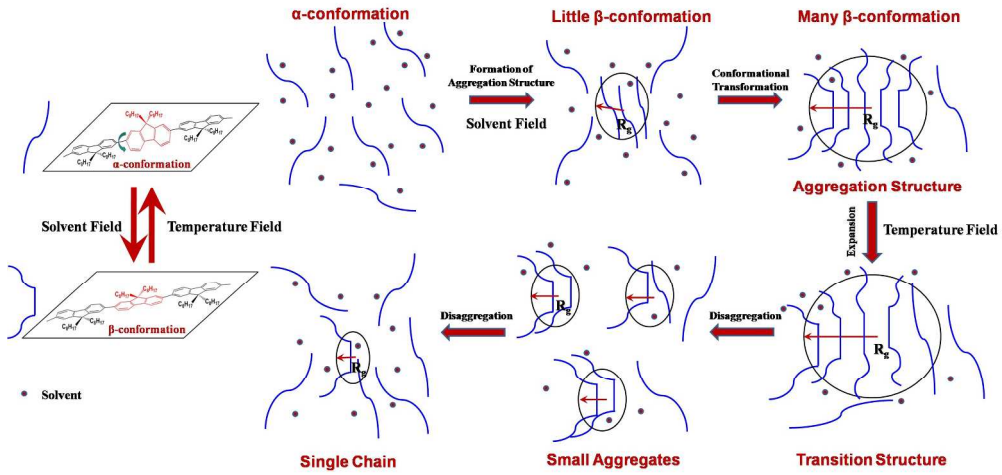

Mutual transformation dynamic process and mechanism between the α-conformation and β-conformation in PFO solution
443x210mm (150 x 150 DPI)

Cite this: DOI: 10.1039/c0xx00000x

www.rsc.org/xxxxxx

ARTICLE TYPE

Transformation Process and Mechanism between the α-Conformation and β-Conformation of Conjugated Polymer PFO in Precursor Solution

Long Huang[a], Tao Li[a], Bo Liu[a], Lili Zhang[a], Zeming Bai[a], Xiaona Li[a], Xinan Huang[a], Dan Lu[a]*

In this work, the solvent field and temperature are used to explore the mutual transformation dynamic process and mechanism between the α-conformation and β-conformation in Poly(9,9-dioctylfluorene) (PFO) precursor solution. The conformational transformation of PFO chain is researched by UV-vis absorption spectra and the proportions of β-conformation are quantitatively calculated. The corresponding variation trend of aggregation structure is researched by using static and dynamic light scattering (SLS/DLS) method. It is found that the mutual transformation process between α-conformation and β-conformation are reversible in essence. Especially in the transformation processes, the complicated relationship between the β-conformation and aggregation structure is understood, that is the aggregation structure make β-conformation formed under solvent field, then the conformational transformation of β-conformation promotes the dissociation of aggregation structure under temperature. The above results give an insight into the β-conformation and aggregation structure of PFO in theory. Furthermore, under the temperature, we find that both two transformation steps have good linear correlations, which indicates that using temperature can be considered as a good method to accurately control the proportion of β-conformation in actual application, and it will help us to get the desired proportion of β-conformation in PFO precursor solution so as to make the charge carrier mobility of optoelectronic films increased and device performance better.

1 Introduction

In recent years, conjugated polymer materials have extensively been used to solar cells, field effect transistors, light-emitting diodes, etc.[1-9] However, some obstacles still need to be overcome before the possible mass industrial production. One of the most limiting factors for device performance is charge carriers mobility. Usually, precursor solution is a determining factor for the properties of devices.[10-12] Therefore, in order to maximize some of the properties of polymer optoelectronic device, a key point is to control the microscopic scale structure (chain aggregation and conformation) of semi-rigid polymer chain in precursor solution.

Because of the outstanding optical and electrical characteristics, PFO has been recognized as an important conjugated polymer material.[13-21] There mainly exist two kinds of chain conformations of PFO, marking as α type and β type.[22] The α type indicates the locally separated chain conformation. While β type describes the weakly ordered domains which can be confirmed by X-ray scattering.[18,21] Moreover, the α type has a smaller intrachain torsion angle than that of the β type, which means that the β type is a more coplanar type, and has an additional local conjugation order state (see Figure 1).[11,12] The β type conformation structure can facilitate charge carrier transport and lead to a higher charge carrier mobility and efficiency of PFO optoelectronics devices.[23,24] Especially, as a "self-dopant" to PFO chain itself,[24,25] β type conformation has great potential as a development target for polymer electrically pumped lasing.[26] Thus based on the presentation in the above paragraph, it is quite essential to research and control the conformation of PFO in precursor solution ahead of the device fabrication.

Following Bradley et al.,[27] many researchers have reported their researches on PFO conformation changing process.[28-36] In recent reports, it can be known that by increasing the intra-chain torsion angle of PFO chain in precursor solution, α type conformation may transform into β type.[10-12] Also, β-conformation can coexist with α-conformation and they can transform into each other in solution.[11,12] However, the detailed

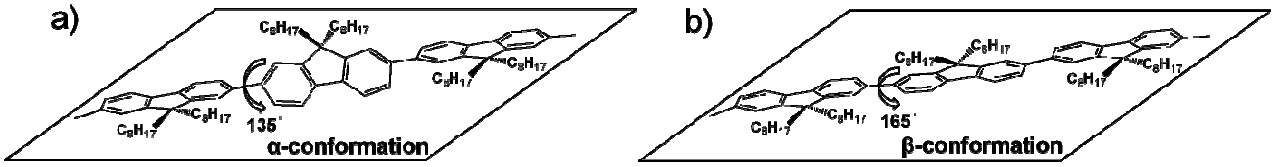

Fig.1 Schematic molecular diagram, (a) The α-conformation of PFO. (b) The β-conformation of PFO.

Cite this: DOI: 10.1039/c0xx00000x

www.rsc.org/xxxxxx

ARTICLE TYPE

transformation mechanism of α and β conformation transformation in solution is not quite clear. Hence, the research on the mutual transformation mechanism between α and β conformation transformation is very critical. In this work, the transformation process and mechanism were studied by two kinds of external fields: solvent field and temperature. The conformational transformation of PFO chain was explored by UV-vis absorption spectra and the proportions of β-conformation were quantitatively calculated. The corresponding variation trend of aggregation structure was explored by light scattering (DLS and SLS). In the process, the conformational transformation and aggregation structure of PFO were controlled smoothly and simply by mixing two perfectly miscible solvents. It was found that the mutual transformation process between α and β conformation were reversible in essence. Especially, the complicated relationship between the PFO β type conformation and aggregation micro-structure in solution was understood, which was still on debate before.[10,11,18,22,37-39]

2. Experimental section

2.1. Materials and the Preparation of Samples.

PFO was bought from American Dye Source, Catalog No.ADS329BE, the weight-average molecular weight (M_w) was 46000 g/mol. Toluene and ethanol were used as good and poor solvent separately, both were bought from Beijing Chemical Company. In the light scattering experiment, the PFO solution with α-conformation and β-conformation mixed together was prepared by following three steps: firstly the PFO was dissolved to solution by the good solvent toluene at 323 K; secondly the PFO solution was filtered directly through Millex Millipore PTFE membrane (0.45 μm) into the light scattering cell; thirdly the poor solvent ethanol which had been filtered before was added into the light scattering cell to induce the β-conformation formed. Finally, the ratios of toluene/ethanol of the PFO solutions were 32:1, 16:1, 8:1, 4:1, 2:1, respectively, and all the concentrations were 0.05 mg mL^{-1}. Also, the PFO aggregation depends on the time elapsed after preparation. So the time between sample preparation and measurements are the same for all samples, which are 5 minutes. For the polymer solution, solvent has a weak stimulation effect on polymer chain as an external filed like electricity, temperature and force, accompanied with an corresponding strong response of the polymer chain (chain conformations or aggregation structure change). In this work, solvent field means using a mixture of good/poor solvent with different ratios, such as 32:1, 16:1, 8:1, 4:1, 2:1.

2.2. The Calculation Method of the Proportion of β-Conformation

The calculation method of the proportion of β-conformation in PFO solution has been reported in our previous researches,[11,12] and it was also presented in Supporting Information.

2.3. Measurements

UV-vis studies were carried out by Shimadzu UV-3000 spectrophotometer. The quartz cuvette was used.

2.4. Light Scattering (LS) Measurements

An ALV/CGS-3 light scattering spectrometer was used in the LS measurements, the spectrometer was equipped with an ALV/LSE-7004 multiple-τ digital correlator and a 22 mW JDS-Uniphase solid-state He-Ne laser (the wavelength was 632.8 nm). The LS cell was put in a thermostat with filtered toluene. In Static LS (SLS), the Rayleigh ratio $R_{vv}(q)$, which leads to the z-averaged root-mean-square radius of gyration R_g of scattering objects was measured, where q is the scattering vector.[40] In dynamic LS (DLS), the intensity time correlation function $g^2(t)$ was measured, where t was the decay time. The $g^2(t)$ could be used to calculated the distribution of relaxation times $G(\tau)$ from the Laplace inversion,[41] the normalized first-order electric field time correlation function $g^1(t)$ could be obtained from the linear fit model $g^1(t)=\int_0^\infty e^{-\tau t}G(\tau)d(\tau)$, and the $g^2(t)$ could be related to $g^1(t)$ from the Siegert relation $g^2(t) = 1 + \beta|g^1(t)|^2$, the details of the LS theory can be seen elsewhere.[42,43]

3. Results and discussion

3.1. Study the Transformation Process and Mechanism from the α type and β type conformation of PFO by the Solvent Field

In the previous research, it was found that the proportion of the β-conformation of PFO can be enhanced significantly by the solvent field, and the percentage of poor solvent ethanol was in the range of 10% to 90%.[11] In this work, a smaller percentage range of ethanol (3.03% to 11.11%) was used to induce the transformation from the α-conformation to β-conformation, the aim is to explore the formation process and mechanism of β-conformation in PFO solution. In Figure 2(a), a normalized UV-vis adsorption spectra is shown, in which five PFO samples dissolved in different ratios of toluene/ethanol are presented. In order to avoid precipitation effects, all the curves were normalized at 405 nm (isobestic point), which has been identified in some articles.[38,44] The peak at 437 nm indicates a exist of β type conformation, while a main band at 391 nm indicates α type conformation.[38] From the ratios of toluene/ethanol 32:1 to 8:1 in PFO solution, the peaks of β-conformation in Figure 2 (a) are very slow. The magnified images of these three curves were presented in the inset. From the inset, with ethanol ratio change, it is clear that the peaks of β type conformation slightly increase, which demonstrates the α type conformation hasn't significantly transform into β-conformation in this stage. While with the ratio of toluene/ethanol varies from 8:1 to 2:1, a sharp rise of the peak of the β type conformation show up, it means that the α-conformation are rapidly transforming into β-conformation.

To better understand the variation trend of β-conformation, the proportions of β-conformation of the five PFO samples were

Cite this: DOI: 10.1039/c0xx00000x

www.rsc.org/xxxxxx

ARTICLE TYPE

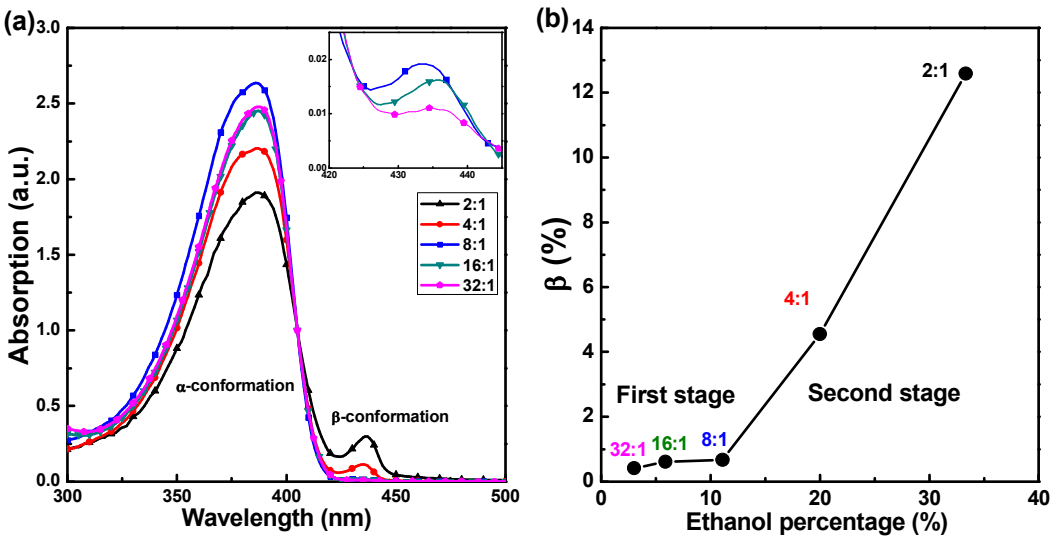

Fig.2 (a) Normalized UV-vis absorption spectra of five PFO samples with different toluene/ethanol ratios: 32:1, 16:1, 8:1, 4:1, 2:1. All the five curves were normalized at the isobestic point (405 nm). The magnified images of 32:1, 16:1 and 8:1 are presented in the inset. (b) The proportions of β-conformation of five PFO samples with different toluene/ethanol ratios: 32:1, 16:1, 8:1, 4:1, 2:1, the error estimates of β-conformation are around 0.03%.

calculated by the method which was reported in the previous researches,[11,12] and they were presented in Figure 2 (b). It can be easily found that from the ratios of toluene/ethanol 32:1 to 8:1 (called as "First stage"), the proportions of β-conformation are around 0.60% and almost do not change with the increasing percentage of ethanol. However, from the ratios of toluene/ethanol 8:1 to 2:1 (called as "Second stage"), the proportions of β-conformation were enhanced rapidly from 0.67% to 12.59%. The experiment can be repeated and the results were similar. This phenomenon is so interesting, and it indicates that the solvent field could not induce a large amount of β-conformation formed if the percentage of ethanol is not high enough. The transformation process and mechanism from the α-conformation to β-conformation arouses our interest, and it will be discussed in detail below. (In supporting information, the corresponding light emission spectra Fig.S1 is well consistent with the UV-vis absorption spectra Fig.2 (a))

The aggregation structure variations of PFO solutions with five toluene/ethanol ratios were measured by DLS. Figure 3(a) shows the autocorrelation function of these solutions. Figure 3 (b) gives their corresponding hydrodynamic radius distribution. In Figure 3 (b), two modes appear. For the 32:1 solution, the fast mode, with the peak of 8 nm, is the PFO single chain (α-conformation), while the slow mode with the peak of 100 nm is the aggregation

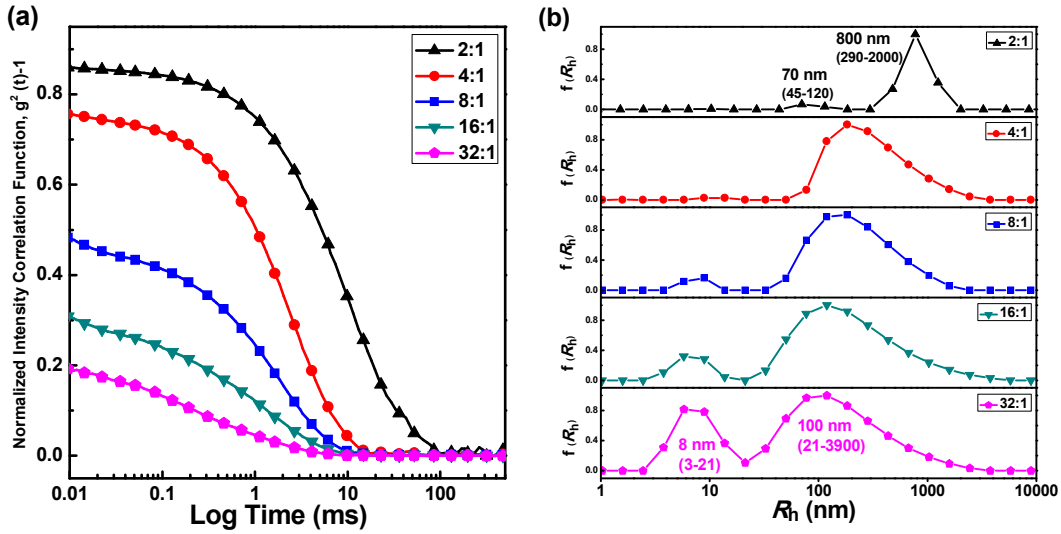

Figure 3 (a) The solvent dependence of autocorrelation functions of the PFO solution, the ratios of toluene/ethanol was 32:1, 16:1, 8:1, 4:1, 2:1, respectively. (b) The corresponding hydrodynamic radius distribution. (θ=40°, T=303 K)

Cite this: DOI: 10.1039/c0xx00000x

www.rsc.org/xxxxxx

ARTICLE TYPE

structure composed of the β-conformation. From the ratios of toluene/ethanol 32:1 to 8:1 ("First stage"), the proportion of the fast mode (α-conformation) decreases with ethanol, and meanwhile the hydrodynamic radius R_h of slow mode increase slightly (i.e. the aggregation degree of PFO increases with ethanol). While from the ratios of 8:1 to 2:1 ("Second stage"), not only the proportion of the fast mode continues decreasing but also its R_h peak increases from 8 nm to 70 nm. While the R_h peak of slow mode increases from 100 nm to 800 nm. It indicates that the aggregation degree of PFO chains becomes higher in "Second stage" than in "First stage". And for the PFO solution of toluene/ethanol the ratio of 2:1, its slow mode 800 nm (290-2000) has the narrower distribution. After repeating the experiment for several times, similar results were got.

The solvent correlation of decay time $<\Gamma>$ between q^2 is shown in Figure 4 (a) and (b), and the slope is the diffusion coefficient D. Diffusion coefficient D reflects the speed of polymer chain in solution. If the D is big, the speed of polymer chain will be fast and the aggregation degree will be low. In contrast, if the D is small, the speed of polymer chain will be slow and the aggregation degree will be high. The experiment results show that the linear relationship between the $<\Gamma>$ and q^2 is good for each PFO solution. The fast mode is the diffusive motion of α-conformation of PFO, while the slow mode should be due to the diffusive motion of aggregation structure in solution. From the ratios of toluene/ethanol 32:1 to 2:1, it can be seen that all the values of D_f and D_s were decreased with ethanol. This result reflects that the aggregation degree is becoming higher with ethanol, which is just consistent with Figure 3 (b).

3.2. Transformation Process and Mechanism from the α-conformation to β-conformation in PFO Solution

Comparing Figure 2 (b) with Figure 3(b), it can be found that the conformational transformation of PFO has a strong correlation with the variation trend of aggregation structure. From the ratios of toluene/ethanol 32:1 to 8:1 ("First stage"), in Figure 2 (b), there is a small amount of the formation of β-conformation. And meanwhile in Figure 3 (b), neither the R_h of the fast mode nor the slow mode change significantly, only the relative proportion of fast mode/slow mode change with ethanol. While from the ratios of toluene/ethanol 8:1 to 2:1 ("Second stage"), in Figure 2 (b), there is a large amount of the formation of β-conformation. And meanwhile in Figure 3 (b), both the R_h of the fast mode and slow mode increase greatly, and the relative proportion of fast mode becomes rather low. The experiment results show that when the percentage of poor solvent ethanol in PFO solution is not high, the ethanol can make the interchain attraction of PFO chains bigger, but it can't supply enough energy to induce the β type conformation formation. Only when the percentage of ethanol reaches a certain value, the PFO α type conformation may transform into β type conformation. Thus, under the solvent field, the transformation process and mechanism from the α-conformation to β-conformation in PFO solution can be depicted, as presented in Figure 5.

In Figure 5, the transformation process and mechanism from the α-conformation to β-conformation can be explained by two stages. In the first stage (from 32:1 to 8:1), the addition of poor solvent ethanol can decrease the interaction between solvent molecule and PFO chain, then it will increase the interchain attraction of PFO chains and make the distance between different chains becomes near, which will lead to the formation of aggregation structure. However, the aggregation degree is not

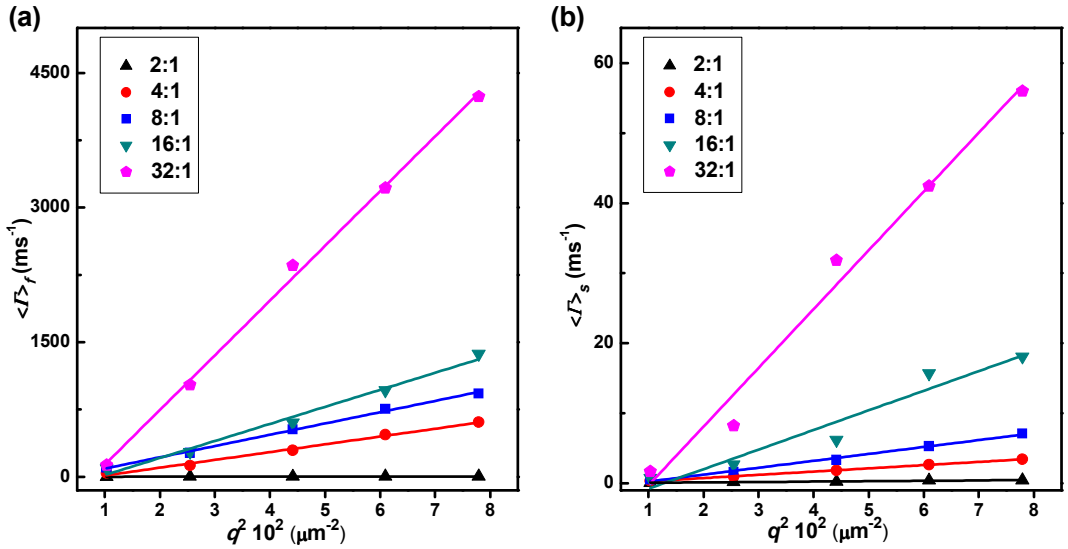

Fig. 4 Solvent dependence of average characteristic line width $<\Gamma>$ vs q^2 in PFO solutions, the ratios of toluene/ethanol was 32:1, 16:1, 8:1, 4:1, 2:1, respectively. (a) the fast diffusive relaxation mode (α-conformation). (b) the slow diffusive relaxation mode (aggregation structure).

Cite this: DOI: 10.1039/c0xx00000x

www.rsc.org/xxxxxx

ARTICLE TYPE

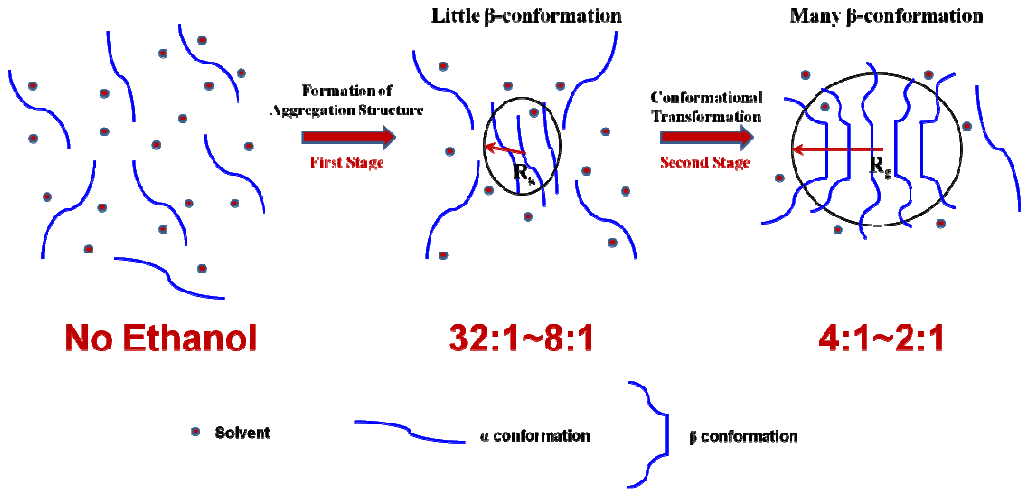

Fig. 5 Transformation process and mechanism from the α type conformation to β type conformation in PFO solution under the solvent field, the ratio of toluene/ethanol is from 32:1 to 2:1.

very high at that time and the distance is also not near enough. According to the interdigitated model,[20] the interaction of side-chain is not able to provide enough energy in this stage for the PFO main chain to overcome the steric hindrance therefore flatten a hierarchical structure (the intrachain torsion angle of β-conformation is 165°, which is more planar than the 135° of α-conformation). Thus the first stage can be considered as a process which is storing up the energy. While in the second stage (from 8:1 to 2:1), the further addition of ethanol can make the aggregation degree become high enough, then the side-chain interaction in aggregation structure can be strong enough to make the PFO backbone planar, namely it will induce the α-conformation transforming into β-conformation largely. Thus from all above, the transformation process and mechanism from the α-conformation to β-conformation under the solvent field has been explained in detail, namely the aggregation structure induces the formation of β-conformation in PFO solution.

3.3. The Proof of Transformation Process and Mechanism from the α-conformation to β-conformation

To prove the rationality of transformation process and mechanism in Figure 5, SLS/DLS was introduced to study the variation trend of R_g, R_h, and R_g/R_h in PFO solution. Here it should be emphasized that R_g represents the root mean square radius of gyration, it reflects the actual size of aggregation structure. R_h is the hydrodynamic radius, it reflects the aggregation degree of PFO chains. The ratio of R_g/R_h is named the form factor, which is used to describe the topological structure and extension state of polymer chains in solution.[12]

Figure 6 shows the solvent dependence of R_g, R_h, and R_g/R_h of these five PFO solutions. It can be seen that both R_g and R_h increases with ethanol, while the form factor R_g/R_h decreases with ethanol. We compared the results in Figure 6 with Figure 5. Firstly in Figure 5, it can be seen that the actual size R_g of aggregation structure indeed becomes bigger, which agrees well with the result of R_g in Figure 6. Secondly, as mentioned above, the interchain attraction in solution will increase with ethanol, which results in a limitation on the movement of PFO chains, so the R_h in Figure 6 becomes bigger. And Figure 5 is just consistent with it. Thirdly, according to the relevant reports,[12,45-50] the structure of polymer chains will be more extended if the R_g/R_h is bigger, and it will be more compact if the R_g/R_h is smaller. In Figure 6, the R_g/R_h decreases with ethanol and reaches the value of 0.15 at last, which indicates that the aggregation structure in PFO solution becomes rather compact. And the corresponding variation trend of aggregation structure in Figure 5 is still well consistent with this trend. Thus, from the results of R_g, R_h, and R_g/R_h in Figure 6, it can be proved that the transformation process and mechanism from the α-conformation to β-conformation in

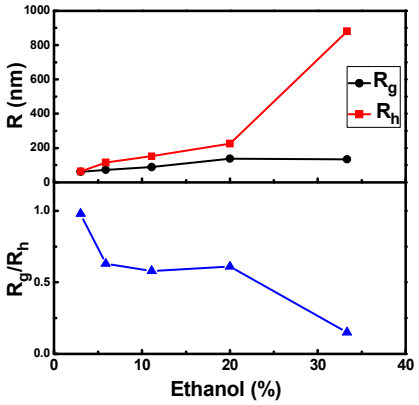

Fig. 6 The solvent dependence of R_g, R_h, and R_g/R_h of PFO solutions, the ratio of toluene/ethanol is from 32:1 to 2:1.

Cite this: DOI: 10.1039/c0xx00000x

www.rsc.org/xxxxxx

ARTICLE TYPE

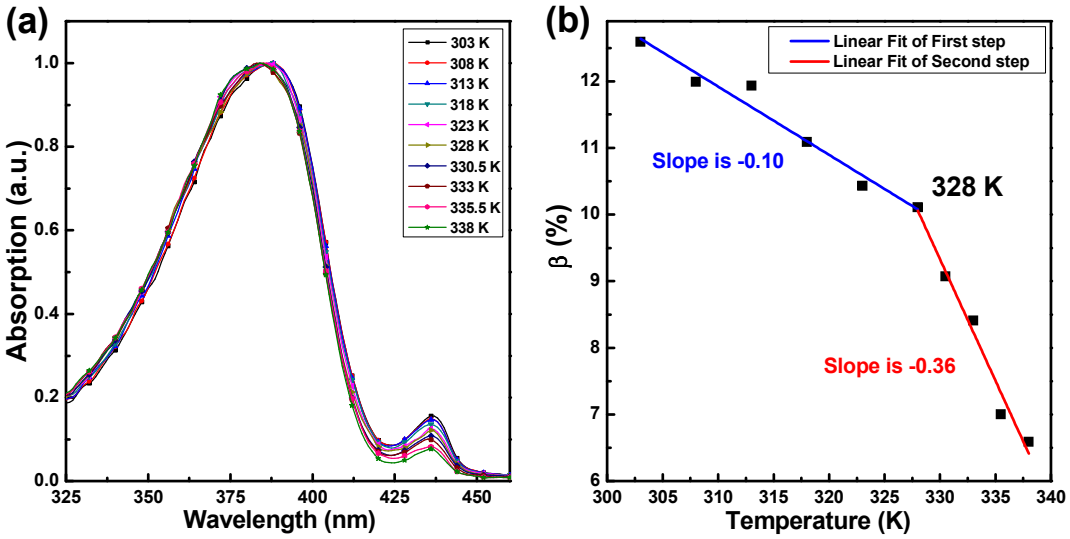

Fig. 7 (a) Normalized UV-vis absorption spectra of PFO solutions at different temperature, the ratio of toluene/ethanol is 2:1 and the temperature range is from 303 K to 338 K. (b) The corresponding proportions of β-conformation with temperature, and they were processed by the piecewise linear fit, and the error estimates of β-conformation are around 0.03%.

Figure 5 is reasonable and credible.

3.4. Study the Transformation Process and Mechanism from the β-conformation to α-conformation by the Temperature

After understanding the transformation process and mechanism from the α-conformation to β-conformation, we want to know if the β-conformation can transform into α-conformation through the opposite process. In the previous report,[12] it was found that the temperature can induce the β-conformation to transform into α-conformation. However, the number of temperature points is too small. In the following study, more temperature points were used to explore the transformation process and mechanism from the β-conformation to α-conformation in PFO solution under the temperature.

In the above study under the solvent field, the ratio of toluene/ethanol is from 32:1 to 2:1. Here the PFO solution with the ratio of 2:1 was chosen as the research object, because its aggregation degree is the highest according to Figure 3 (b) and Figure 4. As shown in Figure 7(a), normalized UV-vis absorption spectra of toluene/ethanol ratio of 2:1 has a temperature dependence, the temperature range is from 303 K to 338 K. With the temperature increase, the peak of β-conformation decreases gradually. To better understand the variation trend of β-conformation, the corresponding proportions of β-conformation with temperature were calculated and they were presented in Figure 7 (b). Figure 7 (b) was processed by the piecewise linear fit. In Figure 7 (b) we can see that the proportion of β-conformation is always decreasing with temperature, which proves that the β-conformation of PFO is transforming into α-conformation gradually in the process. It should be noted that the descent speed of β-conformation below 328 K is different from that above 328 K. To distinguish these two steps, we call them as "First step" and "Second step", respectively. There are good linear correlations between the proportion of β-conformation and the temperature in the both two steps. The value of slope for "First step" is -0.10, while the value of slope for "Second step" is -0.36, namely the descent speed of β-conformation of "Second step" is faster. This phenomenon was so interesting. It was considered that most β-conformation was contained in the aggregation structure of PFO chains, and the aggregation structure could improve the stability of β-conformation,[11] which slowed down the descent speed of β-conformation in the "First step". However, when the temperature is above 328 K ("Second step"), the aggregation structure will disappear gradually, and it leads to the faster transformation from the ordered conformation (β-conformation) to the disordered conformation (α-conformation).

DLS is used to further study the transformation process and mechanism from the β-conformation to α-conformation in PFO solution. It should be noted that there are ten temperature points from 303 K to 338 K in Figure 7 (a) and (b). However, too many points in one figure will make the autocorrelation function unclear, thus we selected six representative points from the ten temperature points, as presented in Figure 8 (a). Figure 8 (a) shows the temperature dependence of autocorrelation functions of the 2:1 PFO solution, and Figure 8 (b) gives their corresponding hydrodynamic radius distribution from 303 K to 338 K. In Figure 8 (a), it can be seen that the autocorrelation functions become steeper gradually with temperature, which reflects that the movement of PFO chains are speeding up and the diffusion coefficient D is increasing. It indicates that the aggregation degree of aggregation structure is decreasing with temperature.

In Figure 8 (b), there are two modes in PFO solution at 303 K.

The fast mode, with a dimension of 70 nm, is a measure of α-conformation, while the slow mode with a dimension of 800 nm is a measure of aggregation structure. From 303 K to 323 K, the peak at 70 nm disappears, and meanwhile a new peak at 200 nm appears. Here we defined a new structure, that is "transition structure", and the new peak is attributed to it. In the heating process, the transition structure is formed by the aggregation structure and the α-conformation together. It can be found that the percentage of the new peak at 200 nm is higher than the previous peak at 70 nm but still lower than the aggregation structure at 800 nm, which indicates that the movement speed of transition structure in PFO solution is faster than the aggregation structure but slower than the α-conformation. From 323 K to 328 K, the span of aggregation structure decreases, and the peak of transition structure is reduced to 100 nm. So it can be known that only a small amount of transition structure is formed from 303 K to 328 K ("First step"), and the aggregation structure still dominates in PFO solution. Especially as mentioned above, the aggregation structure can improve the stability of β-conformation, thus the slower descent speed of β-conformation in "First step" in Figure 7 (b) can be easily understood. From 328 K to 338 K ("Second step"), the peak of aggregation structure is reduced from 800 nm to 180 nm, and the peak of transition structure is reduced from 100 nm to 30 nm. This phenomenon indicates that nearly all the aggregation structure have transformed into the transition structure in this stage, which results in the faster descent speed of β-conformation in "Second step" in Figure 7 (b). Also, the observed aggregate sizes agreed well with the prior research.[18]

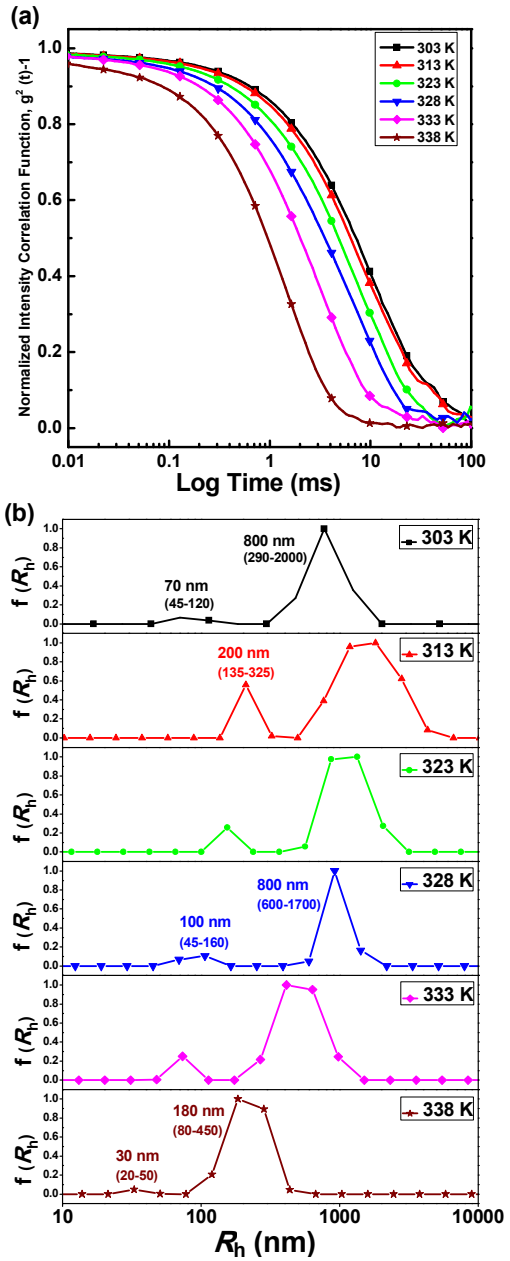

Fig. 8 (a) The temperature dependence of autocorrelation functions of the PFO solution, the ratio of toluene/ethanol was 2:1. Six representative points from the ten temperature points were selected from 303 K to 338 K. (b) The corresponding hydrodynamic radius distribution. (θ=40°)

3.5. Transformation Process and Mechanism from the β-conformation to α-conformation in PFO Solution

SLS/DLS was used to study the transformation process and mechanism of the 2:1 PFO solution under temperature from 303 K to 338 K, as shown in Figure 9. In Figure 9, the R_h of the 2:1 PFO solution decreases with temperature, it reflects that the movement speed of PFO chains is increasing and the aggregation degree is decreasing gradually. The R_g of solution increases from 130 nm to 280 nm with temperature, which indicates that the aggregation structure of PFO chains is expanding gradually, but it always maintains certain geometry and the disaggregation hasn't occur all of the time. The form factor R_g/R_h is increasing with temperature and reaches the value of 1.44 at last, it means that the aggregation structure in PFO solution is becoming more loose and extended. Especially, the rate of increase of R_g/R_h above 328 K ("Second step") is bigger than that below 328 K ("First step"), and this variation trend is just well consistent with both the results in Figure 7 (b) and in Figure 8 (b). Based on the analysis above, the transformation process and mechanism of the 2:1 PFO solution under the temperature can be described here, as presented in Figure 10.

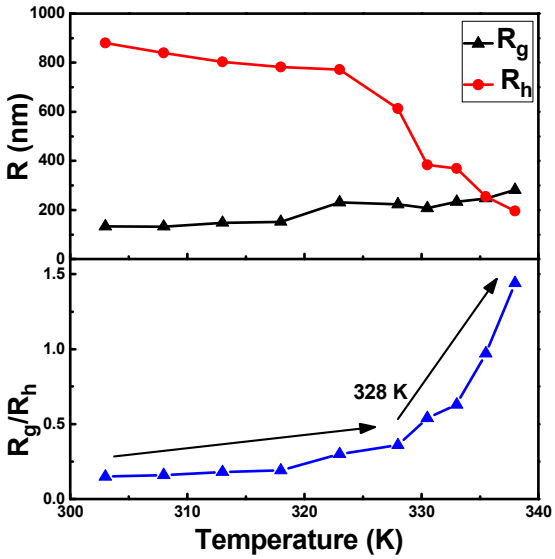

Fig. 9 The temperature dependence of R_g, R_h, and R_g/R_h of the 2:1 PFO solution under the temperature from 303 K to 338 K.

Cite this: DOI: 10.1039/c0xx00000x

www.rsc.org/xxxxxx

ARTICLE TYPE

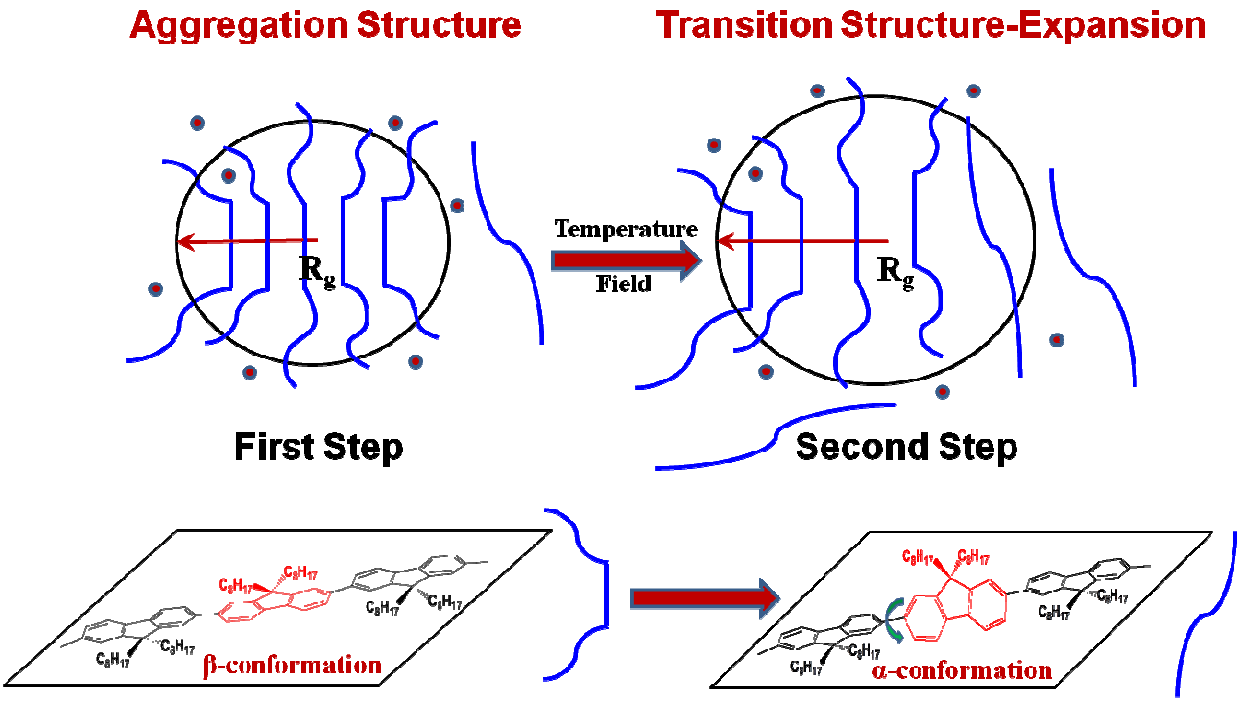

Fig. 10 The transformation process and mechanism of the 2:1 PFO solution under the temperature from 303 K to 338 K.

In Figure 10, the left structure is the compact aggregation structure, and the right structure is the loose transition structure. The β-conformation of PFO can form a local ordered structure[11,18,21,38], just like the structure with parallel arrangement in the figure. While the α-conformation can form a disordered structure, just like the individual locally separated chain in the figure. In the heating process, β-conformation transforms into α-conformation gradually, and meanwhile the aggregation structure will expand to be the transition structure.

For a polymer solution system, the increment of temperature can enhance the chains chaos in solution, it can lead to the transformation of polymer chain from the ordered conformation to disordered conformation. It is just a process in which the conformational entropy will increase. In Figure 10, firstly, temperature rise speeds up the thermal motion of PFO chains and enhance the conformational chaos in solution, it can supply enough free volume for chains to move, which leads to the transformation from β-conformation to α-conformation. So it can be known that in essence, it is the increase of entropy that induces the conformational transformation under the temperature. Secondly, the conformational transformation decreases the interchain attraction of PFO chains, and consequently increase the distance between chains in aggregation structure, which makes the aggregation structure expand to be the transition structure gradually. The expansion of aggregation structure will further promote the β-conformation transform into α-conformation, which well explains the faster descent speed of β-conformation in "Second step" in Figure 7 (b).

From all above, it can be concluded that for the 2:1 PFO solution under temperature, the conformational transformation is the first, then it induce the expansion of aggregation structure. Also, compared to the prior literatures,[18,20,44,51] our proposed mechanism is consistent with that proposed by Bright et al. and Chen et al.

3.6. Further Study on the Transformation Process and Mechanism from the β-conformation to α-conformation by the Temperature

From Figure 9 and Figure 10, we can find that the R_g of solutions always increases with temperature, indicating the transition structure always exists in PFO solution. However, the transition structure is less stable than the aggregation structure, thus we believe that when the energy is high enough, the transition structure should be disaggregated into the single chain at last. Here the PFO solution with the ratio of toluene/ethanol 4:1 was chosen to further study the transformation process and mechanism from the β-conformation to α-conformation under the temperature. It is just because the aggregation degree of the 4:1 PFO solution is smaller than that of the 2:1 PFO solution, based on Figure 3 and Figure 4.

Temperature dependence of the proportions of β-conformation in the 4:1 PFO solution was measured, as shown in Figure 11, in

which the temperature range is from 303 K to 335 K. Figure 11 was also processed by the piecewise linear fit, the same as Figure 7 (b). From Figure 11, it can be known that the proportion of β-conformation is always decreasing with temperature, indicating the β-conformation transforms into α-conformation always in this process. The descent speed of β-conformation below 318 K is different from that above 318 K. To distinguish these two steps, we also call them as "First step" and "Second step", respectively. There are good linear correlations between the proportion of β-conformation and the temperature in the both two steps. The value of slope for "First step" is -0.06, while the value of slope for "Second step" is -0.15, namely the descent speed of β-conformation of "Second step" is faster. This variation trend of β-conformation in Figure 11 is similar to that in Figure 7 (b). Thus it can be deduced that the transition structure also exist in this process, and it will dominate in PFO solution when the temperature is above 318 K ("Second step").

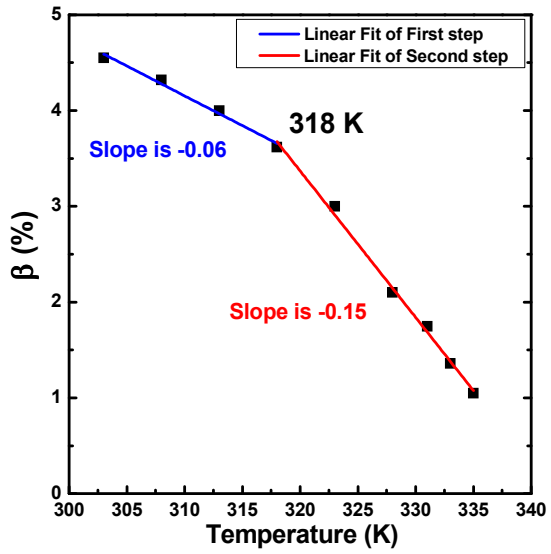

Fig. 11 Temperature dependence of the proportions of β-conformation in the 4:1 PFO solution, the temperature range is from 303 K to 335 K. The figure was also processed by the piecewise linear fit, and the error estimates of β-conformation are around 0.03%.

SLS/DLS was used to study the transformation process and mechanism of the 4:1 PFO solution under the temperature, as shown in Figure 12. In Figure 12, the R_h of the 4:1 PFO solution decreases with temperature, it reflects that the whole aggregation degree of solution is decreasing gradually. From 303 K to 323 K, the R_g of solution increases with temperature. While from 323 K to 335 K, the R_g of solution decreases rapidly with temperature. This phenomenon is different from that of the 2:1 PFO solution in Figure 9. For the 4:1 PFO solution, as mentioned above, when the temperature is above 318 K, the transition structure will dominate in solution. Hence, from 323 K to 335 K, the decrease of R_g should be attributed to the disaggregation of the transition structure, which leads to the disappearance of its certain geometry. And the transition structure disaggregates into many small aggregates in this stage. The form factor R_g/R_h always increases with temperature, which indicates that the structure in PFO solution is becoming looser and looser. Especially, the rate of increase of R_g/R_h becomes bigger when the temperature is above 331 K. R_g/R_h reaches the value of 2.76 at last. According to the relevant reports,[12,45-50] when the value of R_g/R_h is beyond 2.0, the polymer chain is quite extended. Thus it can be considered that the single chains (i.e. α-conformation) dominate at last, and this result agrees well with that in Figure 11, in which there is only 1% β-conformation left at last. Based on the analysis above, the transformation process and mechanism of the 4:1 PFO solution under the temperature can be described here, as presented in Figure 13.

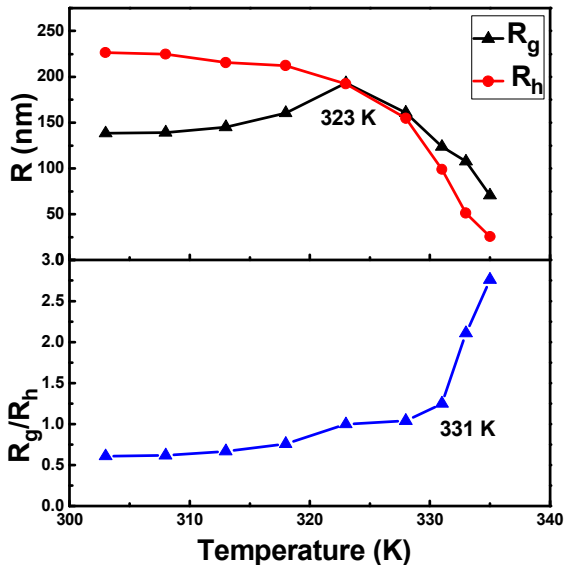

Fig. 12 The temperature dependence of R_g, R_h, and R_g/R_h of the 4:1 PFO solution under temperature from 303 K to 335 K.

As mentioned above, the increment of temperature can enhance the chains chaos in solution, which will lead to the transformation from the ordered conformation to disordered conformation in PFO solution. In Figure 13, firstly from 303 K to 318 K, temperature rise promotes the β-conformation transform into α-conformation, which induces the compact aggregation structure expand to be the loose transition structure gradually. In this stage, the aggregation structure still dominates in solution. Secondly in the range from 318 K to 323 K, based on the variation trend of β-conformation in Figure 11, the transition structure will become dominated in solution this moment. The transition structure continues to expand, but still keeps certain geometry. Thirdly from 323 K to 331 K, more conformational transformations make the interchain attraction of PFO chains weaken significantly, which can't keep the certain geometry of transition structure anymore. Namely the transition structure starts to disaggregate in this stage. The form factor R_g/R_h increases to the value of 1.26 at 331 K, so it can be considered that the transition structure has disaggregated to be many small aggregates. Finally from 331 K to 335 K, the R_g/R_h increase from the value of 1.26 to 2.76, which indicates that nearly all the small aggregates have disaggregated to be the single chains (α-conformation) at last, only few small aggregates left (1% β-conformation).

From all above, the transformation process and mechanism of the 4:1 PFO solution under temperature can be understood.

Cite this: DOI: 10.1039/c0xx00000x

www.rsc.org/xxxxxx

ARTICLE TYPE

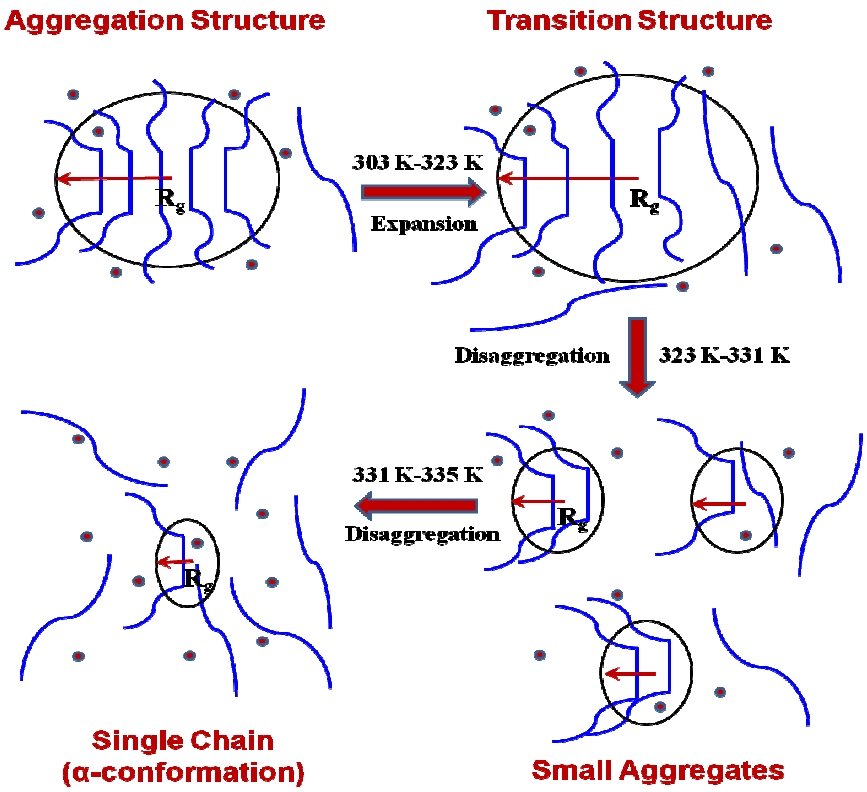

Fig. 13 The transformation process and mechanism of the 4:1 PFO solution under the temperature from 303 K to 335 K.

Temperature rise can enhance the conformational chaos and conformational entropy in PFO solution, and it will lead to the transformation from the ordered conformation (β-conformation) to disordered conformation (α-conformation). Thus in essence, it is a process in which the increase of conformational entropy induces the conformational transformation. Then conformational transformation promotes the aggregation structure to expand to be the transition structure, subsequently the transition structure disaggregates into the small aggregates, and finally into the single chains. Thus, it can be concluded that for the 4:1 PFO solution under temperature, the conformational transformation is the first, then it induce the disaggregation of aggregation structure. Also, compared with the 2:1 PFO solution, the 4:1 PFO solution reflects the whole disaggregation process of aggregation structure, while the 2:1 PFO solution only reflects a section of the process.

As mentioned above in the section 3.2, the transformation process and mechanism from the α-conformation to β-conformation under the solvent field is that the formation of aggregation structure is the first, then it induces the formation of β-conformation in PFO solution. Thus it can be known that the mutual transformation process between the α-conformation and β-conformation in PFO solution are reversible in essence (under the temperature, the range of temperature is from 303 K to 335 K and the equilibrium time of each temperature is 5 minutes). Also in the transformation processes, the complicated relationship between the β-conformation and aggregation structure in PFO solution was understood clearly, which was still on debate before.[10,11,18,22,37-39]

Furthermore, in Figure 7 (b) and Figure 11, it was found that there is good linear correlation no matter in the "First step" or in the "Second step". Also, there is small difference of the proportions of β-conformation between two adjacent temperatures. Thus, the appropriate control of temperature can help us get the desired proportion of β-conformation in PFO precursor solution.

4. Conclusions

In summary, the solvent field and temperature were used to explore the transformation process and mechanism between the α type conformation and β type conformation in PFO precursor solution. For the transformation from the α-conformation to β-conformation under the solvent field, firstly the interchain attraction of PFO chains results in the formation of aggregation structure, then the aggregation structure induces the formation of

β-conformation. For the transformation from the β-conformation to α-conformation under the temperature, firstly the increase of conformational entropy induces the conformational transformation, then the conformational transformation leads to the gradual disaggregation of aggregation structure to the α-conformation. Thus in essence, the mutual transformation process between the α type conformation and β type conformation in PFO solution are reversible. Especially in the transformation processes, the complicated relationship between the aggregation structure and β type conformation in PFO solution was understood clearly. This work gives an insight into the aggregation structure and β type conformation in PFO solution in theory.

Moreover, it was found that the variation trend of β-conformation under the temperature has good linear correlations both in the "First step" and "Second step", which means that using temperature can be considered as a good method to accurately control the proportion of β-conformation. This work is significant in well controlling the proportion of β type conformation in PFO precursor solution, and may have a potential of providing a perpetration method for high speed charge transport material, using for optoelectronic device. We believe the appropriate control of aggregation structure and β type conformation in PFO precursor solution will help us to realize the electrically pumped organic lasing in the future.

Acknowledgments

This work is supported by grants from the National Natural Science Foundation of China (21174049) and (91333103).

Notes and Reference

[a]*State Key Laboratory of Supramolecular Structure and Materials, College of Chemistry, Jilin University, 2699 Qianjin Avenue, Changchun, 130012, China. Tel: +86 431 85167057, Fax: +86 431 85193421; *E-mail: lud@jlu.edu.cn*

† Electronic Supplementary Information (ESI) available: [The calculation method of the proportion of β-conformation in PFO solution, Light emission spectra of the transformation process from α-conformation to β-conformation]. See DOI: 10.1039/b000000x/

1. H. B. Wu, L. Ying, W. Yang and Y. Cao, *Chem. Soc. Rev.*, 2009, **38**, 3391-3400.
2. O. Inganas, F. L. Zhang and M. R. Andersson, *Acc. Chem. Res.*, 2009, **42**, 1731-1739.
3. B. J. Schwartz, *Annu. Rev. Phys. Chem.*, 2003, **54**, 141-172.
4. M. C. Scharber, D. Muhlbacher, M. Koppe, P. Denk, C. Waldauf, A. J. Heeger and C. J. Brabec, *Adv. Mater.*, 2006, **18**, 789-794.
5. Y. Kim, S. Cook, S. M. Tuladhar, S. A. Choulis, J. Nelson, J. R. Durrant, D. D. C. Bradley, M. Giles, I. McCulloch, C. S. Ha, et al., *Nat. Mater.*, 2006, **5**, 197-203.
6. L. L. Chua, J. Zaumseil, J. F. Chang, E. C. W. Qu, P. K. H. Ho, H. Sirringhaus and R. H. Friend, *Nature*, 2005, **434**, 194-199.
7. Y. J. Cheng, S. H. Yang and C. S. Hsu, *Chem. Rev.*, 2009, **109**, 5868-5923.
8. I. Mcculloch , M. Heeney, C. Bailey, K. Genevicius, I. MacDonald, M. Shkunov, D. Sparrowe, S. Tierney, R. Wagner, W. M. Zhang, et al., *Nat. Mater.*, 2006, **5**, 328-333.
9. A. J. Heeger, *Angew. Chem. Int. Ed.* , 2001, **40**, 2591-2611.
10. M. Knaapila and A. P. Monkman, *Adv. Mater.* , 2013, **25**, 1090-1108.
11. L. Huang, X. N. Huang, G. N. Sun, C. Gu, D. Lu and Y. G. Ma, *J. Phys. Chem. C*, 2012, **116**, 7993-7999.
12. L. Huang, L. L. Zhang, X. N. Huang, T. Li, B. Liu and D. Lu, *J. Phys. Chem. B*, 2014, **118**, 791-799.
13. M. Knaapila and M. J. Winokur, *Adv. Polym. Sci*., 2008, **212**, 227-272.
14. A. P. Monkman, C. Rothe, S. M. King and F. B. Dias, *Adv. Polym. Sci.*, 2008, **212**, 187-226.
15. U. Scherf and E. J. W. List, *Adv. Mater*., 2002, **14**, 477-487.
16. S. H. Chen, A. C. Su, C. H. Su and S. A. Chen, *Macromolecules*, 2005, **38**, 379-385.
17. S. H. Chen, H. L. Chou, A. C. Su and S. A. Chen, *Macromolecules*, 2004, **37**, 6833-6838.
18. C. Y. Chen, C. S. Chang, S. W. Huang, J. H. Chen, H. L. Chen, C. I. Su and S. A. Chen, *Macromolecules*, 2010, **43**, 4346-4354.
19. U. Scherf and E. J. W. List, *Adv. Mater*., 2002, **14**, 477-487.
20. D. W. Bright, F. B. Dias, F. Galbrecht, U. Scherf and A. P. Monkman, *Adv. Funct. Mater*., 2009, **19**, 67-73.
21. M. Knaapila, D. W. Bright, R. Stepanyan, M. Torkkeli, L. Almasy, R. Scheweins, U. Vainio, E. Preis, F. Galbrecht, U. Scherf, et al., *Phys. Rev. E* , 2011, **83**, 051803.
22. W. Chunwaschirasiri, B. Tanto, D. L. Huber and M. J. Winokur, *Phys. Rev. Lett.* , 2005, **94**, 107402.
23. J. Peet, E. Brocker, Y. H. Xu and G. C. Bazan, *Adv. Mater*., 2008, **20**, 1882-1885.
24. H. H. Lu, C. Y. Liu, C. H. Chang and S. A. Chen, *Adv. Mater*., 2007, **19**, 2574-2579.
25. M. Ariu, D. G. Lidzey, M. Sims, A. J. Cadby, P. A. Lane and D. D. C. Bradley, J. Phys.: *Condens. Matter* , 2002, **14**, 9975-9986.
26. C. Rothe, F. Galbrecht, U. Scherf and A. P. Monkman, *Adv. Mater*., 2006, **18**, 2137-2140.
27. D. D. C. Bradley, M. Grell, X. Long, H. Mellor, A. W. Grice, M. Inbasekaran and E. P. Woo, *Proc. SPIE*, 1997, **3145**, 254.
28. C. F. Liu, Q. L. Wang, H. K. Tian, J. Liu, Y. H. Geng and D. H. Yan, *Macromolecules*, 2013, **46**, 3025-3030.
29. C. F Liu, Q. L. Wang, H. K. Tian, J. Liu, Y. H. Geng and D. H. Yan, *J. Phys. Chem. B*, 2013, **117**, 8880-8886.
30. A. K. Bansal, A. Ruseckas, P. E. Shaw, I. D. W. Samuel, *J. Phys. Chem. C*, 2010, **114**, 17864-17867.
31. M. J. Tapia, M. Monteserin, H. D. Burrows, J. S. S. de Melo, J. Pina, R. A. E. Castro, S. Garcia and J. Estelrich , *J. Phys. Chem. B*, 2011, **115**, 5794-5800.
32. E. D. Como, K. Becker, J. Feldmann and J. M. Lupton, *Nano Lett*., 2007, **7**, 2993-2998.
33. D. W. Bright, F. Galbrecht, U. Scherf and A. P. Monkman, *Macromolecules* , 2010, **43**, 7860-7863.
34. R. Zhu, G. M. Lin, W. Z. Wang, C. Zheng, W. Wei, W. Huang, Y. H. Xu, J. B. Peng and Y. Cao, *J. Phys. Chem. B*, 2008, **112**, 1611-1618.
35. M. C. Chen, W. C. Hung, A. C. Su, S. H. Chen and S. A. Chen, *J. Phys. Chem. B*, 2009, **113**, 11124-11133.
36. S. H. Chen, A. C. Su and S. A. Chen, *J. Phys. Chem. B*, 2005, **109**, 10067-10072.
37. J. H. Chen, C. S. Chang, Y. X. Chang, C. Y. Chen, H. L. Chen and S. A. Chen, *Macromolecules*, 2009, **42**, 1306-1314.
38. F. B. Dias, J. Morgado, A. L. Macanita, F. P. da Costa, H. D. Burrows and A. P. Monkman, *Macromolecules*, 2006, **39**, 5854-5864.
39. L. L. G. Justino, M. L. Ramos, M. Knaapila, A. T. Marques, C. J. Kudla, U. Scherf, L. Almasy, R. Schweins, H. D. Burrows and A. P. Monkman, *Macromolecules*, 2011, **44**, 334-343.
40. J. Wang, Z. L. Wang, D. G. Peiffer, W. J. Shuely and B. Chu, *Macromolecules*, 1991, **24**, 790-798.
41. C. Wu and K. Q. Xia, Rev. *Sci. Instrum.* , 1994, **65**, 587-590.
42. B. Chu, *Laser Light Scattering*, Academic Press, New York, 1974.
43. B. J. Berne and R. Pecora, *Dynamic Light Scattering*, Plenum Press, New York, 1976.
44. C. C. Kitts and D. A. Vanden Bout, *Polymer* , 2007, **48**, 2322-2330.
45. L. W. Li, C. He, W. D. He and C. Wu, *Macromolecules*, 2011, **44**, 8195-8206.

46. Y. Huang, H. Cheng and C. C. Han, *Macromolecules*, 2011, **44**, 5020-5026.
47. W. Buchard, In *Light Scattering Principles and Development*, Brown, W. Ed. Clarendon Press, Oxford, 1996, p 439.
48. L. J. M. Vagberg, K. A. Cogan and A. P. Gast, *Macromolecules*, 1991, **24**, 1670-1677.
49. W. Burchard, M. Schmidt and W. H. Stockmayer, *Macromolecules*, 1980, **13**, 580-587.
50. J. F. Douglas, J. Roovers and K. F. Freed, *Macromolecules*, 1990, **23**, 4168-4180.
51. M. Knaapila, R. Stepanyan, M. Torkkeli, V. M. Garamus, F. Galbrecht, B. S. Nehls, E. Preis, U. Scherf and A. P. Monkman, *Phys. Rev. E*, 2008, **77**, 051803.

